Numerical Investigation of Single and Multiple Impinging Synthetic Jets on the Flow Field and Heat Transfer at Low Orifice-to-Plate Distances

Eda Ergur
Ph.D. Student
Gazi University
Faculty of Engineering
Mechanical Engineering Dept.
Turkey

Tamer Calisir
Assist. Prof. Dr.
Gazi University
Faculty of Engineering
Mechanical Engineering Dept.
Turkey

In the present numerical study, the thermal performance and fluid flow properties have been investigated to show the effect of single-orifice and multiple-orifice impingement of synthetic jets for dimensionless orifice-to-plate distance (H/D) of lower than one. Investigations have been done for an actuation frequency of f=500 Hz, 0.10 ≤ H/D ≤ 0.75, and dimensionless pitch ratio of 1.25 ≤ D_o/D ≤ 1.75. The results were validated with experimental results from the literature, and a fair agreement was obtained. The results showed that at low nozzle-to-plate spacing, lower target plate temperatures could be obtained. It was observed that with the use of multiple orifices at especially higher D_o/D higher heat transfer values are present. The study was performed to add knowledge to the electronics and aviation industries where high temperatures in small cavities occur.

Keywords: *Impinging synthetic jet, heat transfer, low nozzle-to-plate spacing, electronics cooling, computational fluid dynamics.*

1. INTRODUCTION

Synthetic impinging jets are considered an attractive heat removal technique, which has gradually attracted attention due to some advantages like higher heat transfer in comparison to natural convection, no rotating and moving parts, and no need for complicated piping and pumping [1]. Synthetic jets are called zero-mass-flux systems due to no mass injection. On the other hand, linear momentum is transferred to the fluid [2]. Synthetic jets have been utilized in various applications such as active flow control applications including con–trol of boundary layer transformation/detachment, lift enhancement and drag reduction, underwater vehicle propulsion, heat transfer enhancement by cooling of microprocessors in electronics industry, and mixing augmentation [3, 4]. Especially the development in electronics has led to an increase in heat loads in com–pact volumes. Cooling of the electronic components used in aircraft, unmanned air vehicles, spacecraft, and satellites is vital to maintain efficient use [5]. Within these applications, the cooling of electronic elements in small volumes with less use of components is desired. Hence, synthetic jets are a promising method for the cooling of electronic components in small spaces.

In synthetic jets, a membrane placed on a cavity oscillates which generates flow by causing volume change in the cavity (Fig. 1) [1, 6]. Throughout the oscillating movement of the membrane, the air is ejec–ted and sucked through a nozzle placed at the other end of the cavity [7, 8]. The Reynolds number in synthetic jets is defined as follows.

$$Re = \frac{\rho U_0 D}{\mu} \tag{1}$$

where ρ shows the fluid density, D is the center nozzle diameter, μ shows the dynamic viscosity, and U_0 shows the jet characteristic velocity, which is defined as

$$U_0 = \frac{1}{\tau}\int_0^{\tau/2} u_0(t)\,dt \tag{2}$$

where $u_0(t)$ shows the velocity at the exit plane of the orifice, and τ is the actuation period of jet generation [2].

There exist many studies in the literature considering the heat transfer applications and performance of single and multiple impinging synthetic jets.

Singh et al. [4] investigated the circular synthetic jet impingement heat transfer under different waveforms experimentally. Investigations were performed for dif–ferent Re numbers, dimensionless nozzle-to-plate spacing of 1-25, and frequencies. The effect of stroke length and jet-to-target surface distance (H/D = 2-10) on synthetic jet impingement cooling performance was investigated experimentally by Greco et al. [6]. Chaud–hari et al. [7] examined the heat transfer of a single circular synthetic jet impingement experimentally to obtain the heat transfer performance for various Re numbers, the distance between the jet and impingement surface, and the orifice plate length. The impingement of synthetic jet under various orifice geometries was studied by Singh et al. [8].

Different experiments were done for different Reynolds numbers, orifice plate thicknesses, and jet-to-plate distances. Singh et al. [9] made an investigation to show the effect of sinusoidal and triangular waveforms on synthetic jet impingement under different Re num–bers, H/D=1-18, different frequencies, and stroke leng–

Received: March 2023, Accepted: May 2023
Correspondence to: Dr Tamer Calisir
Gazi University, Faculty of Engineering
06570 Maltepe, Çankaya, Ankara, Türkiye
E-mail: tamercalisir@gazi.edu.tr
doi: 10.5937/fme2303273E

ths. Tan et al. [10] experimentally investigated the syn–thetic jet impingement driven by a piston actuator. They compared the average Nusselt number results between synthetic jets and continuous jets with circular, square, and rectangular orifice geometries. Gil et al. [11] presented experimental results of heat transfer, velocity, and pressure distributions for synthetic impin–ging jets under different Re numbers and Stokes numbers.

Talapati and Hiremath [12] explored the heat transfer of the impingement of synthetic jets under vari–ous frequencies, nozzle diameters, orifice plate thick–nesses, the diameter of the cavity, depth of the cavity, and jet-to-surface gap. Zhang et al. [13] numerically tested the effect of different waveforms on the heat transfer of confined synthetic impinging jets under various Re numbers, orifice-to-plate distances, frequ–encies, and Strouhal numbers. Flow and heat transfer behaviour was studied by Jain et al. [14] to represent the effect of various cavity parameters of a synthetic impinging jet.

Slupski et al. [15] investigated the effect of osci–llation frequency on the sweeping jet experimentally and numerically. They observed that there is a rela–tionship between the inlet mass flow rate and oscillating frequency. In addition, they concluded that the 2D URANS model is a good approximation for the design of sweeping jet actuators.

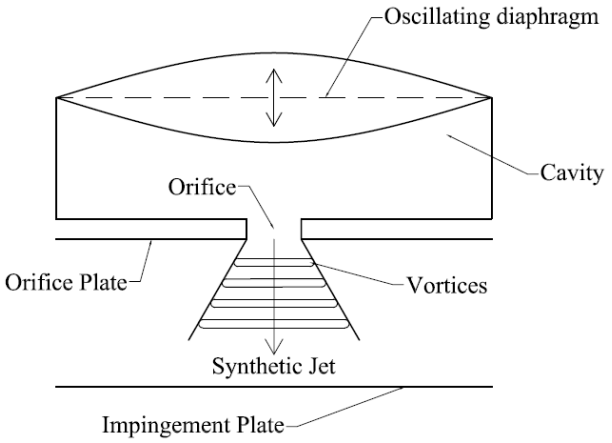

Figure 1. Schematic of a synthetic jet

Also, many studies are present in the literature rep–resenting multiple impinging synthetic jets. Ahmad and Qayoum [3] investigated the heat transfer of synthetic jets under different excitation voltages and frequencies by using one and two orifices. Singh et al. [16] showed the results of a single-orifice and multiple-orifice impinge–ment of a synthetic jet for several orifice geometries. They experimentally compared the thermal performance of single and multiple-orifice synthetic jet impingement under various Re numbers and H/D = 1-25. A compa–rison study was performed for single-ori–fice and multiple-orifice synthetic impinging jet heat transfer and fluid flow by Gil [17]. Experimental mea–surements were carried out by Xiao-Ming and Jing-Zhou [18] to show the synthetic jet impingement cooling performance and flow characteristics from a single cavity with various orifice arrangements. Chaudhari et al. [19] explored the effects of various Re numbers and jet-to-plate gaps (H/D=1-30) by utilizing multiple orifice synthetic jet impingement. The thermal performance of various orifice geometries of the synthetic impinging jet was examined by Mangate et al. [20].

Different Stokes numbers, pitch ratios, and orifice-to-plate distances were taken into account by the researchers. Mangate and Chaudhari [21] investigated the multiple-orifice synthetic jet impingement on a heat sink experimentally. They considered frequency, the distance between orifices, and nozzle-to-plate distance. Particle image velocimetry experiments were performed by Yadav et al. [22] to show the flow of synthetic jets formed from a different number of orifices. Ye et al [23] presented the velocities in the turbulent boundary layer of a synthetic jet array at different locations in the streamwise and spanwise directions.

Fanning et al. [24] experimentally showed the effects of jet-to-plate gap and the distance between orifices for two rectangular synthetic jets. The heat transfer and particle image velocimetry measurement results were presented in the study for H/D = 6 – 24. Paolillo et al. [25] experimentally examined the thermal performance of quadruple-impinging synthetic jets. The effect of various Re and Strouhal numbers was exami–ned by the authors. Kim et al. [26] showed the effect of interaction between two synthetic jets on the flow field. They investigated the effect of the distance between the orifices and stroke length for a fixed Re number. Talapati and Katti [27] experimentally investigated the effect of the temperature of the jet on the heat transfer distribution. Investigations were performed for different frequencies and nozzle-to-surface spacing (H/D=1-8). The effect of waveform shape on the heat transfer and flow characteristics of a single-orifice and multiple-orifice synthetic jet impingements was numerically investigated by Singh et al. [28].

The literature review represents that there have been many experimental as well as numerical studies perfor–med employing single and multiple synthetic impinging jets. Investigations for different orifice-to-plate distan–ces, frequencies, geometries, etc. have been done. How–ever, the investigations are limited to the dimensionless orifice-to-plate distance above 1, where the majority of the range is H/D>2. Hence, there is a lack of infor–mation on synthetic jet impingement flow and heat transfer at low orifice-to-plate distances. This know–ledge is important due to the continual development in the electronics industry, which has led to higher heat loads in smaller volumes. The less need for piping and pumps, and the absence of any rotating part are advantages for synthetic impinging jets in small spaces. Hence, it was aimed to numerically investigate the synthetic jet impingement on a flat plate from a single orifice and multiple circular orifices for H/d $\leq$ 1. The findings could give guidance in the cooling of electronic components used in aviation and space applications, where it is important to maintain less weight with high thermal cooling efficiency.

2. NUMERICAL METHODOLOGY

The problem under investigation has been introduced in this part of the study. In addition, the computation do–main, governing equations, and boundary conditions have been described in detail.

2.1 Computational Domain and Governing Equations

In the present study, the problem under investigation has been built three dimensionally to simulate the impingement of synthetic jets impingement arising from a circular single orifice and multiple orifices as shown in Fig. 2. The cavity is formed with the orifices and an oscillating diaphragm. The height of the cavity is mode–lled as h_c=6.3 mm. The cavity is formed with a square cross-section with extensions (d_c) of 48 mm x 48 mm.

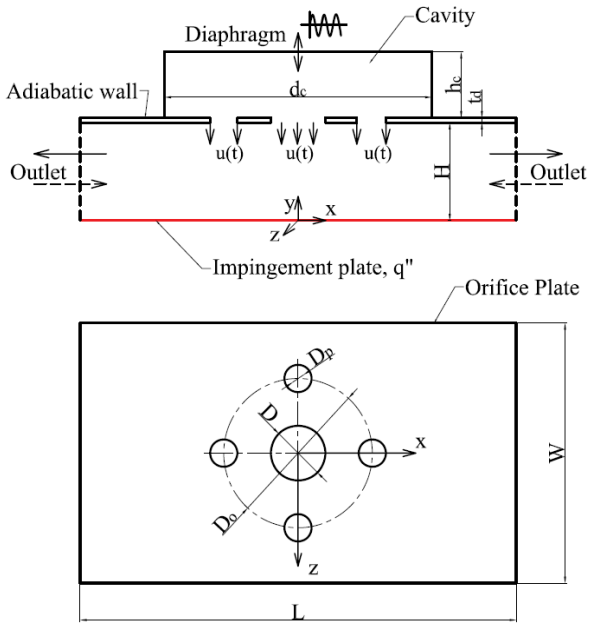

Figure 2. Computational Domain and Boundary Conditions

The diaphragm oscillation creates the synthetic impinging jet which hits a flat target plate that is modelled with a length of L=58 mm and width of W = 53 mm (Fig. 2).

The orifice-to-surface gap (H) is defined as the space among the nozzle exit and the impingement plate. Table 1 summarizes the dimensions of the computa–tional domain. The effect of pitch Diameter (D_o) on heat transfer has been investigated. For this purpose, a range of dimensionless pitch diameters of D_o/D = 1.25 – 1.75 was examined (Fig. 2).

Table 1. Parameters used in the present study.

Parameter	*Value*
Actuation Frequency (f)	500 Hz
Dimensionless orifice-to-plate distance (H/D)	0.10 – 1.00
Pitch diameter ratio (D_o/D)	1.25 – 1.75
Orifice plate thickness (t_d)	2.4 mm
Impingement plate length (L)	58 mm
Impingement plate width (W)	53 mm
Cavity dimension (d_c)	48 mm
Cavity height (h_c)	6.3 mm

Simulations were performed with different nozzle configurations: single circular, and a center orifice with four satellite orifices (see Table 2). The center nozzle was modelled with a diameter of D = 8 mm, and the satellite orifices were modelled with a diameter of 4 mm. The orifice plate has a thickness of t_d = 2.4 mm (Fig. 2).

Table 2. Configurations of the orifices employed in the study.

Configuration	Center diameter (D – mm)	Diameter of Satellite orifices (D_p – mm)	Satellite orifice number
Single	8	-	-
8x4x4	8	4	4

On the impingement plate, a constant heat flux (q" = 1000 W/m^2) was applied, and adiabatic boundary conditions were set on all other walls. The boundary conditions applied on the walls were the no-slip boundary condition. Air at 20°C was used as the fluid. Also, the environmental air temperature was used as 20°C. The pressure boundary condition at the atmospheric pressure was applied at the outlet section. Therefore, an inflow and outflow at the outlet section could occur. The boundary condition applied to the diaphragm has a sinusoidal movement profile and is assumed as a reciprocating piston [9]. The displacement of the diaphragm was modelled time-dependently as follows [1, 14];

$$X(t) = A\sin(2pft) \tag{3}$$

where A (A=200 μm) shows the Amplitude, t is Time, and f is the Frequency, which was applied as f=500 Hz in the present study.

By taking the derivative of Eq. (3), the boundary condition applied to the diaphragm could be obtained [1, 14].

$$U(t) = 2\pi fA\cos(2\pi ft) \tag{4}$$

This equation is used to calculate the speed of the movement of the diaphragm, which forms the velocity inlet boundary condition [1].

The problem under investigation was modelled as time-dependent as a three-dimensional case. The flow was assumed incompressible and turbulent. Viscous dissipation and buoyancy forces were not taken into account. The thermal properties of air like conductivity, viscosity, and density were assumed to be constant. The target surface was heated with a constant heat flux (q"), and investigations of the cooling of the surface by using synthetic impinging jets at low nozzle-to-plate spacing were performed.

Based on these assumptions and simplifications, the mass conservation, momentum, and energy equations are solved in terms of RANS as follows [13, 29, 30, 31];

$$\frac{\partial \overline{u}_i}{\partial x_i} = 0 \tag{5}$$

$$\rho\left(\frac{\partial \overline{u}_i}{\partial t} + \frac{\partial \overline{u_i u_j}}{\partial x_j}\right) = -\frac{\partial \overline{p}}{\partial x_i} + \frac{\partial}{\partial x_i}\left[\mu\left(\frac{\partial \overline{u}_i}{\partial x_i} + \frac{\partial \overline{u}_j}{\partial x_i}\right) - \rho\overline{u_i' u_j'}\right] \tag{6}$$

$$\frac{\partial T}{\partial t}+u_j\frac{\partial T}{\partial x_j}=\alpha\frac{\partial}{\partial x_j}\frac{\partial T}{\partial x_j}-\frac{\partial\overline{u_j'T'}}{\partial x_j} \tag{7}$$

where $-\rho\overline{u_i'u_j'}$ represents the Reynolds stresses.

To enclose the above equations, the Boussinesq assumptions are accepted which are given as follows;

$$-\rho\overline{u_i'u_j'}=\mu_t\left(\frac{\partial u_i}{\partial x_j}+\frac{\partial u_j}{\partial x_i}\right)-\frac{2}{3}\rho k\delta_{ij} \tag{8}$$

where μ_t, shows the eddy viscosity, k is representing turbulent kinetic energy [28].

In the present study, the FloEFD CFD software was employed to numerically investigate synthetic jet im–pingement heat transfer and fluid flow.

To determine the turbulent quantities, the Lam-Bremhorst k-ε turbulence model was utilised in the study. In the k-ε model, empirical additions were emp–loyed [33]. In this turbulence model, damping functions were used to obtain a better boundary profile [33]. The equations representing the model are presented.

$$\rho\frac{\partial k}{\partial t}+\rho\overline{u}_i\frac{\partial k}{\partial x_i}=\frac{\partial}{\partial x_i}\left[\left(\mu+\frac{\mu_t}{\sigma_k}\right)\frac{\partial k}{\partial x_i}\right]+ +\mu_t\left(\frac{\partial\overline{u}_i}{\partial x_j}+\frac{\partial\overline{u}_j}{\partial x_i}\right)\frac{\partial\overline{u}_i}{\partial x_j}+G_k-\rho\hat{\varepsilon} \tag{9}$$

$$\rho\frac{\partial\varepsilon}{\partial t}+\rho\overline{u}_i\frac{\partial\hat{\varepsilon}}{\partial x_i}=\frac{\partial}{\partial x_i}\left[\left(\mu+\frac{\mu_t}{\sigma_k}\right)\frac{\partial\hat{\varepsilon}}{\partial x_i}\right]+ +f_1C_1\mu_t\frac{\hat{\varepsilon}}{k}\left(\frac{\partial\overline{u}_i}{\partial x_j}+\frac{\partial\overline{u}_j}{\partial x_i}\right)\frac{\partial\overline{u}_i}{\partial x_j}+C_1G_k-f_2C_2\rho\frac{\hat{\varepsilon}}{k} \tag{10}$$

where μ_t shows the turbulent kinetic energy, C_μ, C_1, and C_2 are constant coefficients in the model. The turbulent Prandtl numbers have been represented with σ_k and σ_ε.

The damping functions used in the model are determined by [32];

$$f_\mu=\left[1-\exp\left(-0.0165\,\mathrm{Re}_y\right)\right]^2\left(1+\frac{20.5}{\mathrm{Re}_t}\right) \tag{11}$$

$$f_1=\left(1+\frac{0.05}{f_\mu}\right)^3 \tag{12}$$

$$f_2=1-\exp\left(-\mathrm{Re}_t^2\right) \tag{13}$$

where Re_t and Re_z show the turbulent Reynolds num–bers.

2.2 Data Reduction

In the present study, the synthetic jet impingement of single and multiple orifices on a flat target surface under constant heat flux has been investigated, and the results have been presented in the form of time-averaged local heat transfer coefficient (h) and Nusselt number (Nu), which are evaluated as follows;

$$h=\frac{q''D}{k\left(T_p-T_0\right)} \tag{14}$$

$$Nu=\frac{hD}{k}=\frac{q''D}{k\left(T_p-T_0\right)}. \tag{15}$$

where T_p and T_o show the time-averaged local surface temperature and air temperature, respectively.

The time and area-averaged Nusselt number (Nu_{avg}) and heat transfer coefficient (h_{avg}) could be calculated by replacing T_p in Eq. (14) and Eq. (15) with the time and area-averaged temperature on the impingement surface.

2.3 Mesh and Time Step Independency Study

Reliable results of the parametric study could be obtained by independency studies for mesh and time step by taking f=500 Hz and H/D = 1.00 as an example case. As shown in Table 3, five different mesh numbers are used to acquire mesh independency. A systematic increase was applied in x × y × z directions to show the change in heat transfer with mesh number. Table 3 summarizes the time and area-averaged heat transfer coefficient on the target plate. The mesh values represent the grid numbers in the x × y × z directions. It is obvious that the highest deviation was around 3% between Case 1 and Case 2. Afterwards, the relative deviation between the cases was around 1%, which is enough to justify when the mesh number is higher than 80 × 80 × 80. In addition, it was observed that the computational time and computational sources increased by almost 30% and 21%, respectively, with the increase in mesh number from 80 × 80 × 80 to 88 × 88 × 88. Hence, by taking computational accuracy and sources into account, the grid with the 80 × 80 × 80 mesh number was selected to carry out further solutions.

Table 3. Grid independency study.

Case	Mesh number	Time and area-averaged heat transfer coefficient (h_{avg})
1	65×65×65	44.14
2	72×72×72	42.79
3	80×80×80	43.19
4	88×88×88	42.56
5	96×96×96	42.12

The mesh structure used within the study has been presented in Fig. 3. To capture the impingement heat transfer and flow structure in the vicinity of the target surface, a more dense mesh was applied above the surface. Hence, the requirement of y+ < 1 was satisfied.

In addition, a time-step independency study has been performed by using the mesh number of 80 × 80 × 80, and the results are listed in Table 4. The time steps have been chosen to satisfy the Courant-Friedrichs-Lewy (CFL) number below 1. The CFL was obtained by using the average jet exit velocity and the mesh number of 80 × 80 × 80. It was observed that the time step should be less than 5.7×10^{-5} (i.e. $\tau/35$). Four kinds of time steps such as $\tau/100$, $\tau/250$, $\tau/400$, and $\tau/800$ were employed to define the suitable time step. Table 4 represents that there is a small change in the heat transfer coefficient,

where τ/250 was selected for all simulations in the parametric study. As can be seen from the results, the deviation between τ/250 and τ/400 is small enough, and hence the time step of τ/250 is regarded as adequate for all simulations.

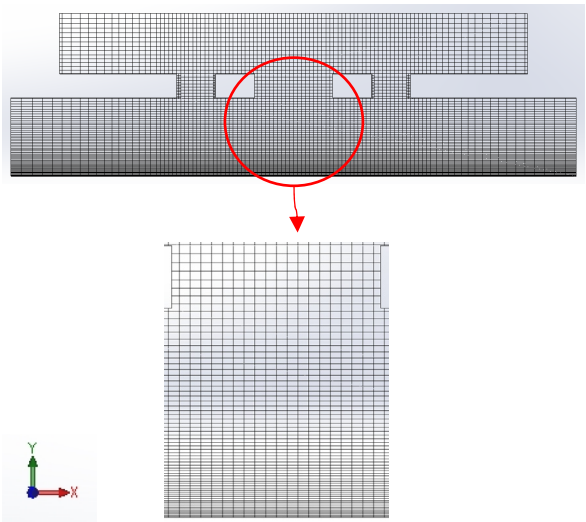

Figure 3. Mesh structure used in the study

Table 4. Time independency study.

Case	Time and area-averaged heat transfer coefficient (h_{avg})
τ/100	65.07
τ/250	65.48
τ/400	63.89
τ/800	66.03

2.4 Validation of the numerical model

The numerical results obtained for the single orifice as well as multiple orifices have been validated with experimental results from the literature. The results for the single-orifice case were validated by using the findings of Chaudhari et al. [7] for various frequency values at H/D=4. The comparison results have been presented in Fig. 4. It was observed that the results are in general in agreement with the experimental findings of Chaudhari et al [7] except for the frequency of f=200 Hz, where a deviation of 17.9% has been obtained. It was observed that the flow field and temperature distribution for f=150 Hz and f=200 Hz are similar, which shows close results in the average heat transfer coefficient. Afterwards, a sudden increase was obser–ved. This was attributed to a transition value in the frequency which could not be captured by the turbu–lence model within this range. Hence, a higher deviation was observed for f=200 Hz. On the other hand, a fair agreement was obtained for the remaining frequency values.

Also, validation for the multiple-orifice case has been performed, and the numerical results have been validated with the experimental results of Singh et al. [8] for various H/D values under f=150 Hz. Fig. 5 represents that a fair agreement with the experimental results has been obtained.

It could be mentioned that the results obtained for the single-orifice as well as the multiple-orifices are valid.

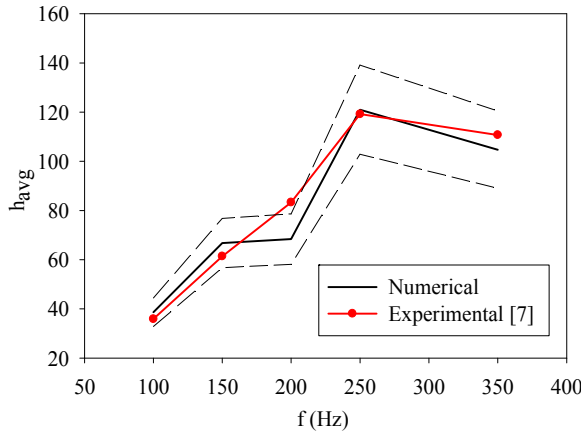

Figure 4. Validation of single-orifice for various frequencies at H/D=4 with the results of Chaudhari et al. [7]

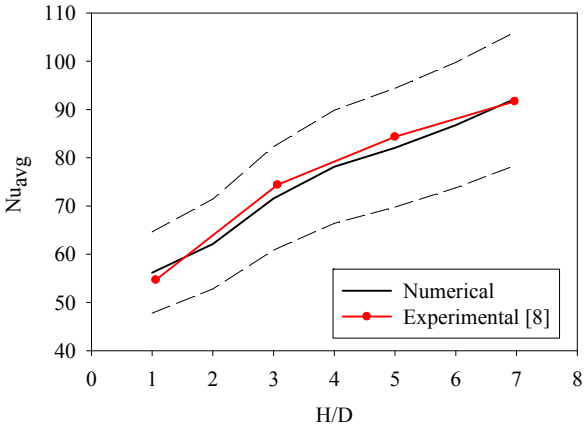

Figure 5. Validation of multiple-orifice for various H/D at f=150 Hz with the results of Singh et al. [8]

3. RESULTS AND DISCUSSION

In this part of the study, the numerical results were shown for single-orifice and multiple-orifice synthetic impinging jets under H/D=0.10 – 1.00, D_o/D = 1.25 – 1.75, and f = 500 Hz. The overall aim was to present and add knowledge in the field of synthetic impinging jets at low nozzle-to-plate distances for single- and multiple-orifice impinging synthetic jets. Hence, the flow characteristics and the heat transfer performance were shown for impinging synthetic jets at H/D≤1.00.

To understand the flow behaviour and to interpret the thermal results of multiple-orifice synthetic impin–ging jets at low nozzle-to-plate distances, streamlines and velocity contours at f=500 Hz actuation frequency and various D_o/D values for orifice-to-plate distances of 0.15 and 0.75 are shown for different time intervals in Fig. 6 and Fig. 7, respectively. Due to symmetry, only the right half of the domain is shown in the Figures 6-7. At time t=0, the fluid ejected from the cavity at maximum velocity, and the velocity decreased until t=0.4τ when the suction phase began. Fig. 6 shows that in the discharge phase, two clockwise vortexes occurred in the cavity due to the cavity geometry. It was noted that especially the vortex above the center orifice deflected the flow; hence, higher velocities were observed close to the side surfaces of the orifices. Thus, lower velocities were seen at the x=0 location during the ejection phase. Therefore, lower heat transfer was

expected around the stagnation point. The impingement under the satellite orifices occurred at higher velocities due to the smaller diameter of the satellites, where during the ejection phase (t=0 – 0.2τ), a clockwise vortex was formed along the height of the channel at the near side of the center orifice. It could be observed that this vortex blocks the wall jet flowing from the center orifice. This will have a decreasing effect on heat transfer at this region for all investigated D_o/D values. The suction phase begins at the time t=0.4τ and continues until t=0.8τ. As one can see, with the start of the suction phase, vortexes occur in the cavity region, and at t=0.6τ, two vortexes are present in the cavity. Also, when t=0.6τ during the suction phase near the stagnation region of the center as well as satellite orifices anticlockwise vortexes occur. These vortexes have a blocking effect on the fresh air (cold air) coming from the outlet section into the cavity. This could have a decreasing influence on heat transfer due to the decrease in cold air entering the cavity. When t=0.8τ, the flow is sucked into the cavity within the center orifice, which creates a major clockwise vortex in the cavity. This vortex leads the air to satellite orifices where ejection occurs. Hence, the air is sucked through the center orifice and ejected through the satellite orifices and impinges on the target surface. After the impingement through the satellite orifices when t=0.8τ, the air is directed towards the outlet, as well as to the center orifice although a moderate increase in heat transfer could occur due to the impingement through the satellite orifice. At this time step, heated air is circulated through the cavity, which could result in a decreased heat transfer.

The time-dependent velocity distribution for H/D=0.75 is shown in Fig. 7. At time t=0, air impinges on the target surface at the highest velocity, and a decrease in velocity occurs at t=0.2τ. At that moment, vortexes occur near the outlet region of the channel. These vortexes have a blocking effect on the wall jets, especially for D_o/D=1.25. However, at t=0.4τ the suction of fresh air to the cavity starts, and for D_o/D>1.25, a large anticlockwise vortex occurs, which has a blocking effect on the fresh air (cold air). In addition, the heated air is mixed with the fresh air; hence, the temperature increases in the cavity, which has a degrading effect on heat transfer. This large vortex is present at t=0.6τ – 0.8τ for D_o/D=1.75.

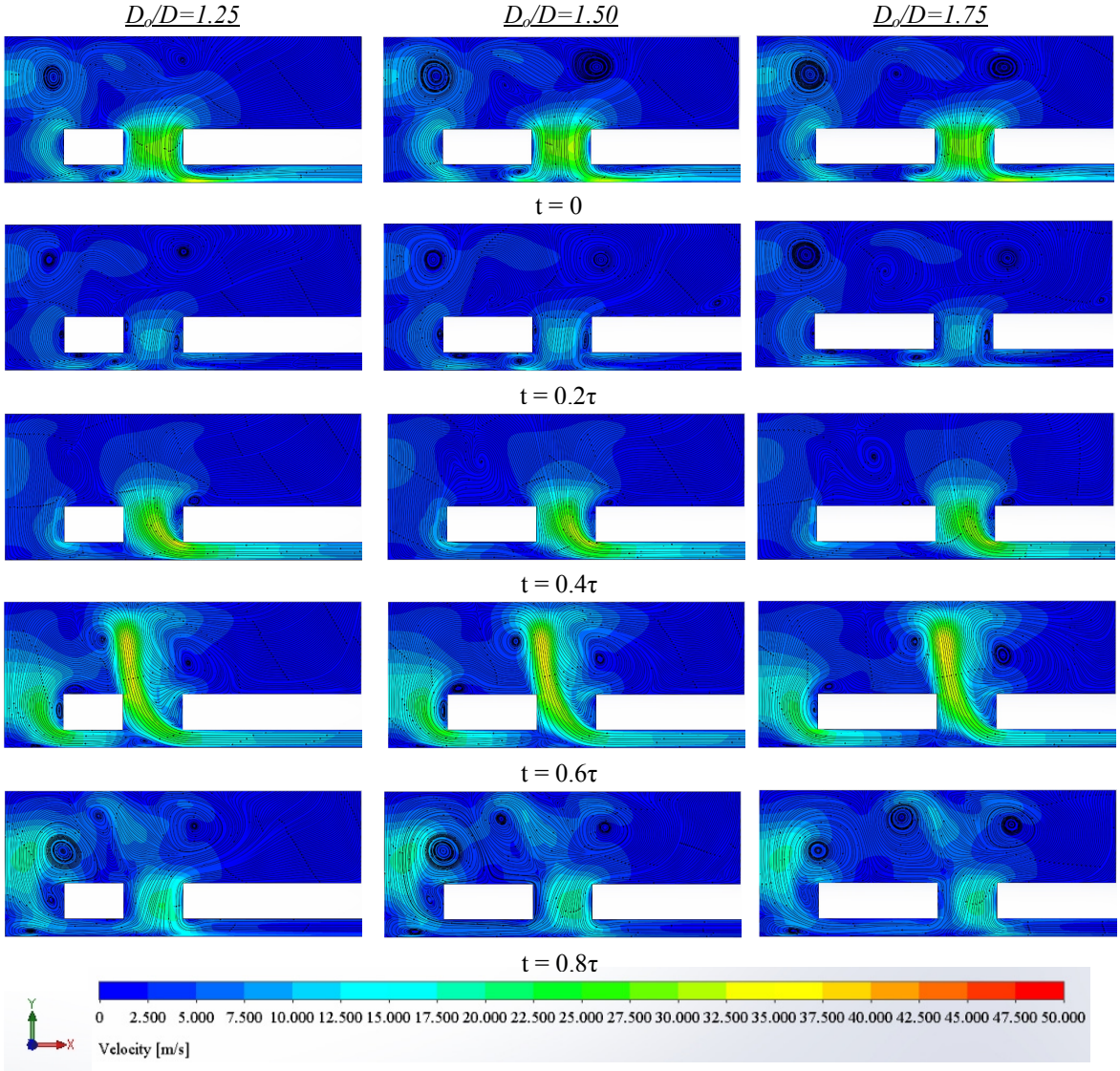

Figure 6. Velocity contours and streamlines for H/D=0.15 under various D_o/D.

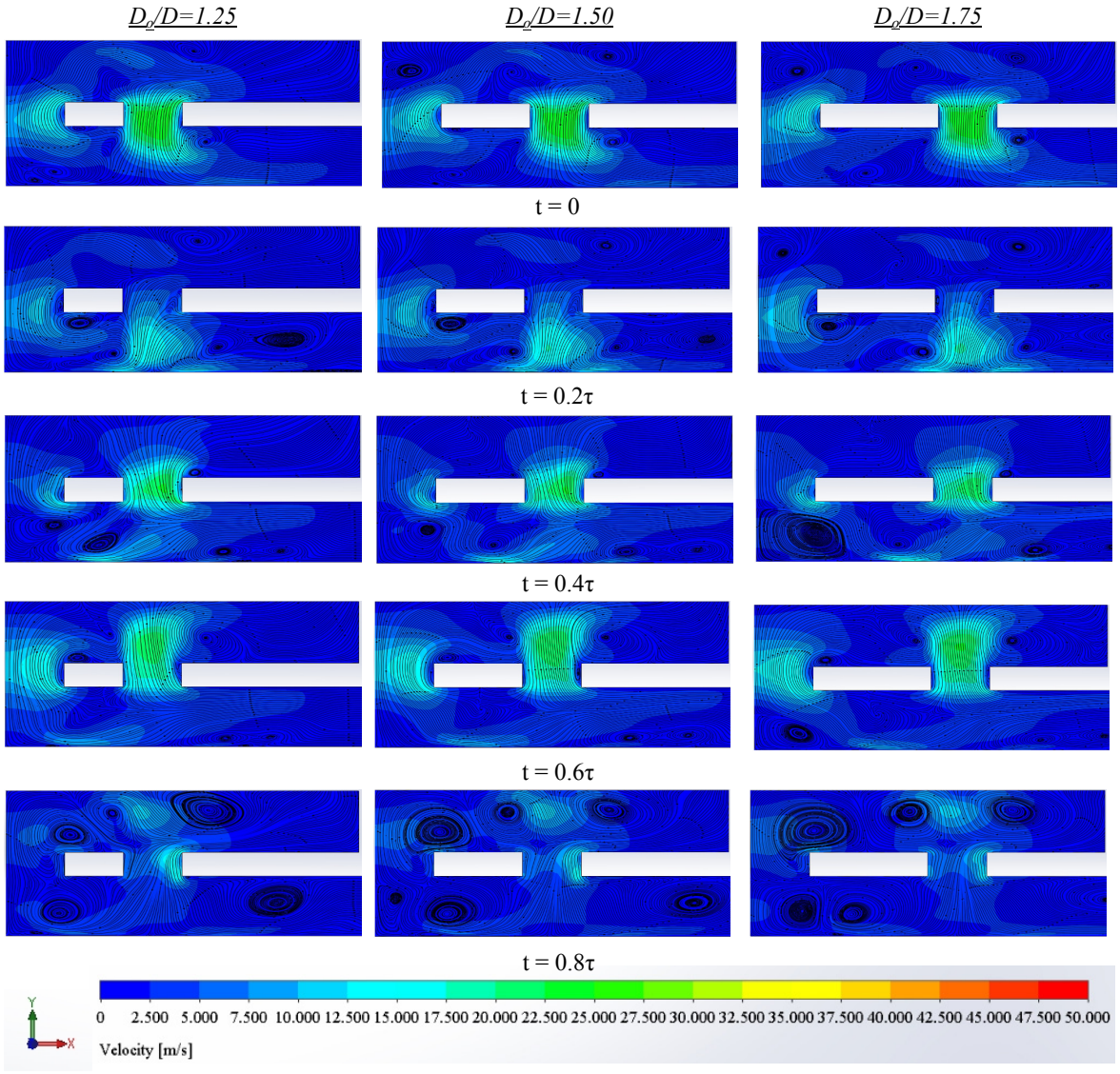

Figure 7. Velocity contours and streamlines for H/D=0.75 under various D_o/D.

On the other hand, at t=0.8τ, a large anticlockwise vortex is found below the center orifice for all D_o/D. The vortex around the impingement region causes mixing with the cold fluid which enters from the outlet. Hence, an increase in the temperature inside the cavity occurs.

Afterwards, the heat transfer performance of the single-orifice and multiple-orifice impinging synthetic jet has been shown. Fig. 8 – Fig. 10 shows the time-averaged local Nu number distributions for nozzle-to-orifice distances of 0.15, 0.50, and 0.75, respectively. The results were shown for various D_o/D values.

As one can see from the figures, the highest stagnation point Nu number under the center orifice is obtained for the single nozzle. This is attributed to the fact that the vortexes at that region below the center orifice increase the air temperature; thus, a decrease in heat transfer in the region of $0.0 \leq x/D \leq 0.5$ occurs. On the other hand, for the multiple-orifice case at H/D=0.15 (Fig. 8), a sudden increase in Nu number occurs, and the highest Nu number values are obtained below the center of the satellite orifices. Also, the maximum Nu number values are moving towards the outlet with the increase in D_o/D.

In addition, a considerable augmentation in heat transfer is observed with the increase in D_o/D, which is attributed to the interaction of the jets with the decrease in D_o/D with a degrading effect on heat transfer (Fig. 6). Although a small maximum region occurs when H/D=0.15 (Fig. 8), a wider maximum region has been observed with the increase in H/D. This is attributed to the widening and development of the jet with the increase in H/D. As can be seen for H/D=0.50 and H/D=0.75, a minimum heat transfer region occurs around x/D=0.75 for D_o/D=1.75. This shows that the vortexes in the mid-region of the orifices have a degrading effect on heat transfer (Fig. 7).

The heated air recirculates at this region, and prevents fresh air (cold air) to enter the cavity. Hence, a decrease occurs.

The temperature distribution occurring on the target plate for single-orifice and multiple-orifice has been presented for various H/D values in Fig. 11. As one can see, the lowest temperatures occur at low orifice-to-plate distances, which is because of the high momentum of the jet. This causes high momentum in the wall jet region, which has an increasing effect on heat transfer. Conversely, the impingement regions of the satellite

nozzles could be observed distinctly, whereas the impingement region of the center jet could be hardly observed. This is not the case for the single orifice, where the impingement region becomes wider by growing the gap between the nozzle and plate. In addition, at higher orifice-to-surface distances, the impingement regions under satellite orifices widen, which is in agreement with Fig. 9 and Fig. 10. Besides, at high nozzle-to-plate distances and low D_o/D values, due to the lowering in jet momentum, higher temperature values are observed at the corner of the target plate. In general, it could be concluded that lower temperature values have been observed for multiple-nozzle, especially at higher D_o/D.

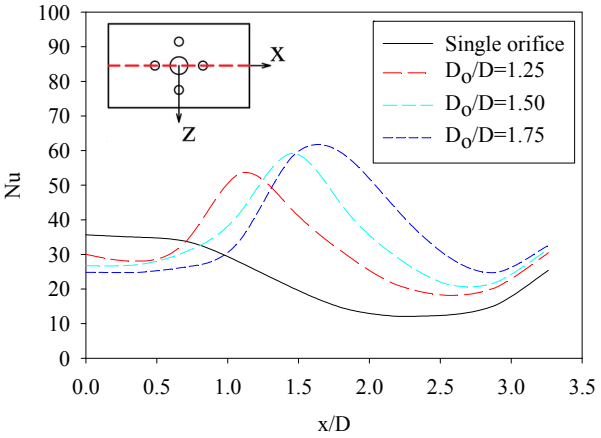

Figure 8. Variation of local Nu number under different nozzle configurations at H/D=0.15

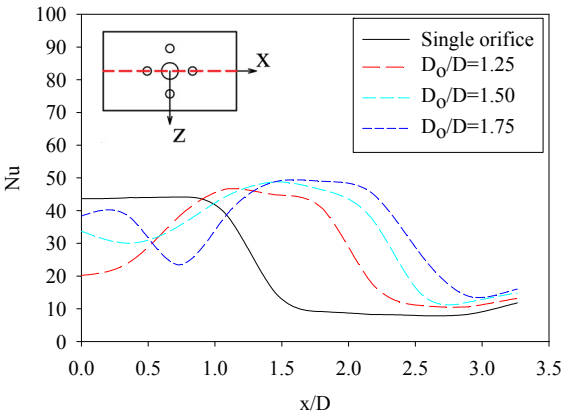

Figure 9. Variation of local Nu number under different nozzle configurations at H/D=0.50

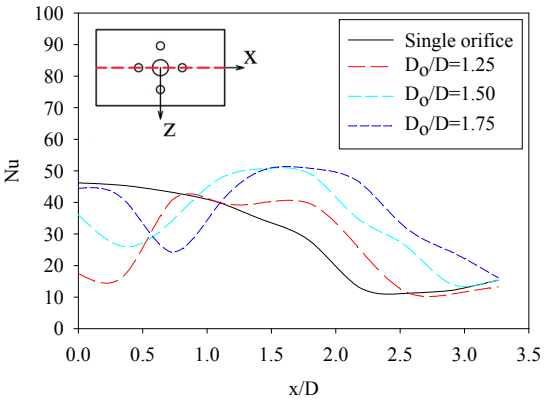

Figure 10. Variation of local Nu number under different nozzle configurations at H/D=0.75

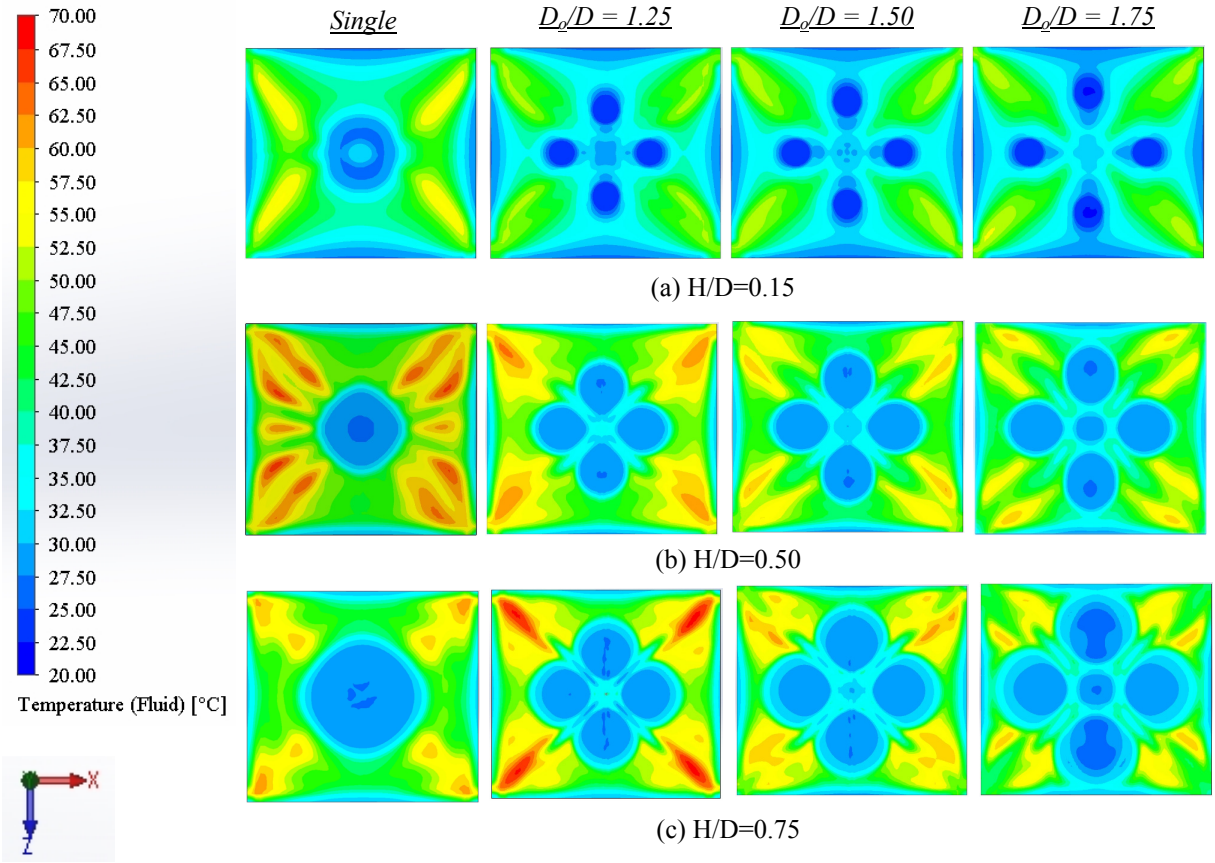

Figure 11. Temperature contours on the target surface for various H/D and D_o/D values.

The variation in time and area-averaged Nu number (Nu_{avg}) with respect to H/D for several dimensionless pitch diameters (D_o/D) is shown in Fig. 12. The findings are compatible with Fig. 11. It is observed that the least heat transfer has been seen for the single-orifice within the limits of $0.10 \leq H/D \leq 0.50$.

On the other hand, within the limits of $0.10 \leq H/D < 0.50$, the average heat transfer results for multiple orifices are close for all D_o/D. This is due to the high momentum of the jets at low nozzle-to-plate spacing, which provides high heat transfer rates. In addition, the flow field at low nozzle-to-plate spacing is less affected by the dimensionless pitch diameter (D_o/D). However, for $H/D > 0.50$, the heat transfer for D_o/D=1.25 and 1.50 remains almost constant, whereas a high increase rate has been observed by using a single orifice in a similar range of nozzle-to-plate spacing.

In the range of $0.75 \leq H/D \leq 1.00$, an increase of around 23% has been obtained in heat transfer for the single-orifice case. This is attributed to the widening of the jet with an increase in nozzle-to-plate spacing, where it is possible to cool a larger area (Fig. 11). On the other hand, with the increase in nozzle-to-plate spacing and at low pitch diameters, the heat transfer drops due to the jet interaction, which is also observed in Fig. 11.

4. CONCLUSIONS

Synthetic jet impingement flow and heat transfer have been investigated numerically to show the effect of a single-orifice and multiple-orifices at low nozzle-to-plate spacing and dimensionless pitch ratios. Simulations were done for f=500 Hz, H/D = 0.10 – 1.00, and D_o/D=1.25 – 1.75. In this direction, the problem under investigation has been first validated with experimental studies from the literature, and a good agreement has been obtained. Afterwards, a parametric study has been done.

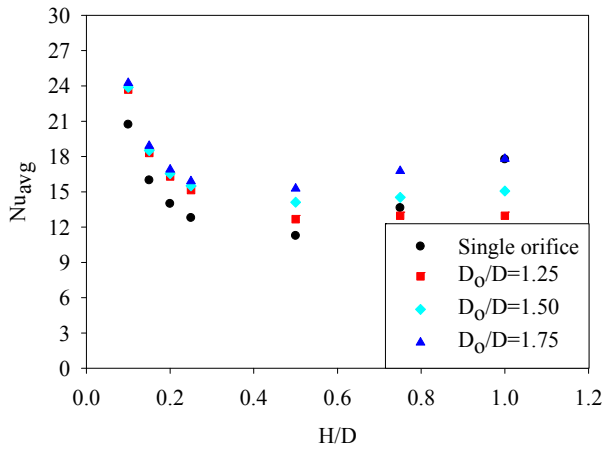

Figure 12. Nu_{avg} for different nozzle configurations at various H/D

The overall aim was to present and add knowledge in the field of synthetic impinging jets at low nozzle-to-plate distances for single- and multiple-orifice-impinging synthetic jets. The findings could be concluded as follows:

- The flow field was affected by the number of orifices, and with the increase in nozzle-to-plate spacing and decrease in dimensionless pitch diameter, jet interaction increased, which has a degrading effect on heat transfer.
- In general, higher stagnation point Nu number values were obtained for the single-orifice case.
- On the other hand, the highest Nu number values were obtained below the satellite orifices.
- The decrease in H/D led to lower target plate temperatures due to the high momentum of the jet impinging on the target plate.
- The increase in D_o/D could provide lower target plate temperatures.
- Lowest Nu_{avg} values were obtained for single-orifice within the limits of $0.10 \leq H/D \leq 0.50$. In the same range, the average heat transfer results for multiple-orifices were close for all D_o/D.
- For H/D=1.00, almost the same Nu_{avg} values were obtained for the single-orifice and multiple-orifice with D_o/D.

In addition, some future projections about the study could be mentioned as follows:

- The sinus profile has been used in the present study to activate the membrane. Recently, some studies exist on the effect of the activation membrane. Hence, the effect could be investigated for the present geometry and boundary conditions.
- A constant frequency of f=500 Hz has been implemented in the present study. However, the effect of different activation frequencies would give insight into the flow and heat transfer at low nozzle-to-target distances for multiple synthetic impinging jets.
- Although the implemented turbulence model in the present study shows a fair agreement in general, the use of different turbulence would be important, especially in the solution of the vortexes occurring in the flow field of synthetic jets.

ACKNOWLEDGMENT

The authors gratefully acknowledge the financial support of this study by the research fund of Gazi University under Grant No. FYL-2021-7213. The authors also would like to thank Gazi University Academic Writing Application and Research Center for proofreading the article.

REFERENCES

[1] Yu, Q., Mei, Z., Bai, M., Xie, D., Ding, Y., Li, Y.: Cooling performance improvement of impingement hybrid synthetic jets in a confined space with the aid of a fluid diode, Applied Thermal Engineering, Vol. 157, pp. 113749, 2019.

[2] Smith, B.L., Glezer, A.: The formation and evolution of synthetic jets, Physics of Fluids, Vol. 10, No. 9, pp. 2281-2297, 1998.

[3] Ahmad, M., Qayoum, A.: Investigation of Impingement of Double Orifice Synthetic Jet for Heat and Fluid Flow Characteristics in Quiescent Flow, Pertanika J. Sci & Technol., Vol. 27, No. 3, pp. 1181-1206, 2019.

[4] Singh, P.K., Renganathan, M., Yadav, H., Sahu, S.K., Upadhyay, P.K., Agrawal, A.: An experi–

mental investigation of the flow-field and thermal characteristics of synthetic jet impingement with different waveforms, International Journal of Heat and Mass Transfer, Vol. 187, pp. 122534, 2022.

[5] Elhefnawy, A., Elmaihy, A., Elweteedy, A.: A University Small Satellite Thermal Control Modeling and Analysis in the Post-Mission Phase, FME Transactions, Vol. 49, pp. 1014-1024, 2021.

[6] Greco, C.S., Paolillo, G., Ianiro, A., Cardone, G., de Luca, L.: Effects of the stroke length and nozzle-to-plate distance on synthetic jet impingement heat transfer, International Journal of Heat and Mass Transfer, Vol. 117, pp. 1019-1031, 2018.

[7] Chaudhari, M., Puranik, B., Agrawal, A.: Heat transfer characteristics of synthetic jet impingement cooling, International Journal of Heat and Mass Transfer, Vol. 53, pp. 1057-1069, 2010.

[8] Singh, P.K., Sahu, S.K., Upadhyay, P.K., Jain, A.K.: Experimental investigation on thermal characteristics of hot surface by synthetic jet impingement, Applied Thermal Engineering, Vol. 165, pp. 114596, 2020.

[9] Singh, P.K., Sahu, S.K., Upadhyay, P.K., Singh S.: Experimental and numerical investigation of the thermal performance of impinging synthetic jet with different waveforms, Experimental Heat Transfer, Vol. 36, No. 2, pp. 121-142, 2023.

[10] Tan, X.M., Zhang, J.Z., Yong, S., Xie, G.N.: An experimental investigation on comparison of synthetic and continuous jets impingement heat transfer, International Journal of Heat and Mass Transfer, Vol. 90, pp. 227-238, 2015.

[11] Gil. P., Wilk, J., Smusz, R., Galek, R.: Centerline heat transfer coefficient distributions of synthetic jets impingement cooling, International Journal of Heat and Mass Transfer, Vol. 160, pp. 120147, 2020.

[12] Talapati, R.J., Hiremath, N.S.: Optimization of thermal characteristics of axisymmetric synthetic air jet impingement on flat surface, Journal of Mechanical Engineering and Sciences, Vol. 16, No. 3, pp. 9129-9141, 2022.

[13] Zhang, Y., Li, P., Xie, Y.: Numerical investigation of heat transfer characteristics of impinging synthetic jets with different waveforms, International Journal of Heat and Mass Transfer, Vol. 12, pp. 1017-1027, 2018.

[14] Jain, M., Puranik, B., Agrawal, A.: A numerical investigation of effects of cavity and orifice parameters on the characteristics of a synthetic jet flow, Sensors and Actuators A: Physical, Vol. 165, pp. 351-366, 2011.

[15] Slupski, B.J., Tajik, A.R., Parezanovic, V.B., Kara, K.: On the Impact of Geometry Scaling and Mass Flow Rate on the Frequency of a Sweeping Jet Actuator, FME Transactions, Vol. 47, pp. 599-607, 2019.

[16] Singh, P.K., Sahu, S.K., Upadhyay, P.K.: Experimental investigation of the thermal behaviour a single-cavity and multiple-orifice synthetic jet impingement driven by electromagnetic actuator for electronics cooling, Experimental Heat Transfer, Vol. 35, No. 2, pp. 132-158, 2022.

[17] Gil, P.: Flow and heat transfer characteristics of single and multiple synthetic jet impingement cooling, International Journal of Heat and Mass Transfer, Vol. 201, pp. 123590, 2023.

[18] Xiao-Ming, T., Jing-Zhou, Z.: Flow and heat transfer characteristics under synthetic jets impingement driven by piezoelectric actuator, Experimental Thermal and Fluid Science, Vol. 48, pp. 134-146, 2013.

[19] Chaudhari, M., Puranik, B., Agrawal, A.: Multiple orifice synthetic jet for improvement in impingement heat transfer, International Journal of Heat and Mass Transfer, Vol. 54, pp. 2056-2065, 2011.

[20] Mangate, L., Yadav, H., Agrawal, A., Chaudhari, M.: Experimental investigation on thermal and flow characteristics of synthetic jet with multiple-orifice of different shapes, International Journal of Thermal Sciences, Vol. 140, pp. 344-357, 2019.

[21] Mangate, L.D., Chaudhari, M.B.: Experimental study on heat transfer characteristics of a heat sink with multiple-orifice synthetic jet, International Journal of Heat and Mass Transfer, Vol. 103, pp. 1181-1190, 2016.

[22] Yadav, H., Joshi, A., Chaudhari, M., Agrawal, A.: An experimental study of a multi-orifice synthetic jet with application to cooling of compact devices, AIP Advances, Vol. 9, pp. 125108, 2019.

[23] Ye, Z., Jiang, Y., Zhang, Y., Zou, J., Zheng, Y.: Effects of Synthetic Jet Array on Turbulent Boundary Layer, International Journal of Heat and Technology, Vol. 37, No. 3, pp. 893-898, 2019.

[24] Fanning, E., Persoons, T., Murray, D.B.: Heat transfer and flow characteristics of a pair of adjacent impinging synthetic jets, International Journal of Heat and Fluid Flow, Vol. 54, pp. 153-166, 2015.

[25] Paolillo, G., Greco, C.S., Cardone, G.: Impingement heat transfer of quadruple synthetic jets, International Journal of Heat and Mass Transfer, Vol. 135, pp. 1192-1206, 2019.

[26] Kim M., Lee, H., Hwang, W.: Experimental study on the flow interaction between two synthetic jets emanating from a dual round orifice, Experimental Thermal and Fluid Science, Vol. 126, pp. 110400, 2021.

[27] Talapati, R.J., Katti, V.V.: Influence of synthetic jet air temperature on local heat transfer characteristics of synthetic air jet impingement, International Communications in Heat and Mass Transfer, Vol. 130, pp. 105796, 2022.

[28] Singh, P.K., Shah, A.K., Tripathi, S.N., Yadav, H., Upadhyay, P.K., Sahu, S.K.: Numerical investigation of the flow and thermal behaviour of impinging single and multi-orifice synthetic jets with different waveforms, Numerical Heat

Transfer, Part A: Applications, Vol. 83, No. 6, pp. 573-593, 2022.

[29] Li, P., Huang, X., Guo, D.: Numerical analysis of dominant parameters in synthetic impinging jet heat transfer process, International Journal of Heat and Mass Transfer, Vol. 150, pp. 119280, 2020.

[30] Baliti, J., Hssikou, M., Elguennouni, Y., Moussaoui, A., Alaoui, M., Heat Transfer and Entropy Generation for Natural Convection by Adiabatic Obstacles Inside a Cavity Heated on the Left Side, FME Transactions, Vol. 48, pp. 825-832, 2020.

[31] Ahamad, N.A., Kamangar, S., Aljohani, A.F., Azeem, Baig, M.A.A., Badruddin, I.A., Double Diffusion in Square Porous Cavity Subjected to Conjugate Heat Transfer, FME Transactions, Vol. 48, pp. 841-848, 2020.

[32] Simcenter: *Simcenter FloEFD Technical Reference – Software Version 2022.1*, January 2022.

[33] Mentor Graphics: *Enhanced Turbulence Modelling in FloEFD*, 2011.

NOMENCLATURE

A	Amplitude
c_p	Specific heat
C	Coefficient
d_c	Cavity dimension
D	Diameter of center orifice
D_o	Pitch diameter
D_p	Diameter of satellite orifice
f	frequency
f_1,f_2,f_μ	Damping functions
h	heat transfer coefficient
H	orifice-to-plate distance
k	conduction coefficient
Nu	Time-averaged Nu number
Nu_{avg}	Time and area averaged Nu number
q"	Heat flux
Re	Re number
T	Temperature
t	Time
u_0	Velocity at the exit plane of the orifice
U_0	Characteristic velocity
Vy	Time-averaged axial velocity
W	Width of impingement plate
X(t)	Displacement of the diaphragm
x,y,z	Coordinates

Greek symbols

α	Thermal diffusivity
δ_{ij}	Kronecker delta
ε	Dissipation rate of turbulent kinetic energy
μ	Dynamic viscosity
μ_t	Eddy viscosity
ν	Kinematic viscosity
ρ	Density
τ	Actuation period of jet generation

Superscripts

avg	time and area-averaged

НУМЕРИЧКО ИСПИТИВАЊЕ ПОЈЕДИНАЧНИХ И ВИШЕСТРУКИХ УДАРА СИНТЕТИЧКИХ МЛАЗОВА НА ПОЉЕ ПРОТОКА И ПРЕНОС ТОПЛОТЕ НА МАЛИМ РАСТОЈАЊИМА ИЗМЕЂУ ОТВОРА И ПЛОЧЕ

Е. Ергур, Т. Калисир

У овој нумеричкој студији, термичке перформансе и својства протока флуида су истраживани да би се показао ефекат удара синтетичких млазова са једним отвором и са више отвора на растојање између отвора и плоче (Х/Д) мање од један. Истраживања су рађена за фреквенцију активирања од ф=500 Хз, 0,10 ≤ Х/Д ≤ 0,75 и бездимензионални однос корака од 1,25 ≤ До/Д ≤ 1,75. Резултати су потврђени експерименталним резултатима из литературе и постигнуто је поштено слагање. Резултати су показали да се при малом размаку између млазница и плоча могу постићи ниже температуре циљне плоче. Уочено је да су при употреби вишеструких отвора при посебно већим До/Д присутне веће вредности преноса топлоте. Студија је спроведена како би се додало знање у електронску и авио-индустрију где се јављају високе температуре у малим шупљинама.